NASA Technical Memorandum 81230

Effect of Winglets on the Induced Drag of Ideal Wing Shapes

R. T. Jones and T. A. Lasinski

September 1980

National Aeronautics and Space Administration

1. Report No.	2. Government Accession No.	3. Recipient's Catalog No.
NASA TM-81230		

4. Title and Subtitle	5. Report Date
EFFECTS OF WINGLETS ON THE INDUCED DRAG OF IDEAL WING SHAPES	6. Performing Organization Code

7. Author(s)	8. Performing Organization Report No.
R. T. Jones and T. A. Lasinski	A-8329
	10. Work Unit No. 505-31-11-08

9. Performing Organization Name and Address	11. Contract or Grant No.
Ames Research Center, NASA Moffett Field, CA 94035	

12. Sponsoring Agency Name and Address	13. Type of Report and Period Covered
National Aeronautics and Space Administration Washington, D.C. 20546	Technical Memorandum
	14. Sponsoring Agency Code

15. Supplementary Notes

16. Abstract

A conventional wing having a given lift and a limited span achieves minimum induced drag when the spanwise distribution of lift is elliptical. However, if the limitation on span is removed and replaced by a structural constraint on the integrated bending moments, Prandtl found that a 10-percent reduction of induced drag can be achieved by a 10-percent increase of wing span accompanied by a more highly tapered loading. In the present report, we have extended such calculations to wings having vertical tip extensions or winglets. It is found that essentially the same result can be obtained by a 15-percent vertical extension. Thus, it appears that with ideal wing shapes similar reductions of induced drag can be achieved by either horizontal or vertical tip extensions.

17. Key Words (Suggested by Author(s))	18. Distribution Statement
Aerodynamics Wings Winglets Tip extensions	Unlimited STAR Category — 02

19. Security Classif. (of this report)	20. Security Classif. (of this page)	21. No. of Pages	22. Price*
Unclassified	Unclassified	29	

*For sale by the National Technical Information Service, Springfield, Virginia 22161

NASA Technical Memorandum 81230

Effect of Winglets on the Induced Drag of Ideal Wing Shapes

R. T. Jones
T. A. Lasinski, Ames Research Center, Moffett Field, California

National Aeronautics and
Space Administration

Ames Research Center
Moffett Field, California 94035

EFFECTS OF WINGLETS ON THE INDUCED DRAG OF IDEAL WING SHAPES

R. T. Jones and T. A. Lasinski

Ames Research Center

It has been known for many years that vertical fins or end plates at the tips of a wing can significantly reduce vortex drag. Recent work (ref. 1) has shown considerable improvement over earlier designs and has raised the question of whether such vertical extensions should be a part of the basic design of a wing intended for maximum efficiency.

The answer to such a question depends on several factors, but most importantly on the weight of the wing structure. As is well known, the requirements of minimum vortex drag and minimum structure weight are almost directly opposed. To minimize the vortex drag, the wing system must have either large lateral or large vertical dimensions — leading to a heavy structure.

If we assume that the wing weight depends only on the dimensions and is independent of details of the lift distribution, we are led to the problem originally solved by Munk (ref. 2), that is, minimum vortex drag for a given total lift and given span. Munk's problem was later extended by Hemke (ref. 3) to include the effect of vertical tip fins. In references 4 and 5, Faulkner and Darwin determine the distribution of lift for wings with fins having minimum drag with given dimensions.

In addition to their dependence on the absolute dimensions, the wing weight and vortex drag will depend to a certain extent on the distribution of lift or side force over the wing system. In 1933, Prandtl (ref. 6) considered this aspect of the problem and sought to determine the spanwise lift distribution for minimum drag with a fixed wing weight as well as a given total lift and given span. Prandtl assumed that a fraction of the weight of the wing structure is proportional to the bending moment integrated over the whole span. For a planar wing the average or integrated value of the bending moments turns out to be just the second moment or "moment of inertia" of the load curve. Prandtl's criterion seems more appropriate than the criterion used by one of the present writers (see ref. 7) in which only the bending moment at the wing root was considered.

If we relax the restriction on the absolute dimensions of the wing and consider a family of wings having the same total lift and the same integrated bending moment, but varying in span, Prandtl's solution shows that the vortex drag can be reduced by about 10 percent when compared with that of the elliptic wing. Figure 1 shows one of the wing shapes obtained by Prandtl's method compared with an elliptic wing. We have assumed that each section operates at the same lift coefficient, so that the chord distribution is proportional to the load distribution. It is interesting that such a narrow tip extension can reduce the vortex drag by 10 percent.

To extend Prandtl's analysis to nonplanar wings, we have to consider not only the spanwise lift distribution but also the varying inclination of the lift vectors along the length of the wing. Figure 2 shows a nonplanar wing in front view and illustrates the notation. Positions along the span are denoted by arc length s and angle θ or by rectangular coordinates y and z. Using a customary notation, the local "lift" force normal to the curved wing surface will be

$$\ell(s,\theta) = \rho V \Gamma(s) \tag{1}$$

where Γ is the circulation and

$$\Gamma = \Delta\phi \tag{2}$$

is the jump in potential ϕ across the wake in the Trefftz plane behind the wing. With these definitions the total lift L will be

$$L = \int_{-s_t}^{+s_t} \rho V \Gamma \cos\theta \, ds \tag{3}$$

where s_t denotes the wing tip; the drag, D_i, is given by

$$D_i = \int_{-s_t}^{+s_t} \rho \frac{w}{2} \Gamma \, ds \tag{4}$$

where w is now the component of the induced "downwash" in the direction normal to the curved wing plane. In the integration for the drag the downwash at the wing is taken as one-half the final value in the Trefftz plane. For the bending moment at a station s_o, y_o, z_o we have

$$M(s_o) = \int_{s_o}^{s_t} \rho V \Gamma [(y - y_o)\cos\theta + (z - z_o)\sin\theta] ds \tag{5}$$

and the bending moment integrated over the arc length of the wing spars will be

$$\bar{M} = \int_{o}^{s_t} M(s_o) ds_o \tag{6}$$

We are now in a position to find the condition for minimum drag with a given structural constraint such as $\bar{M}$. This is, of course, a problem in the calculus of variations, but since the drag D_i is simply a quadratic function in the space of load distributions it is not necessary to employ sophisticated techniques. Assume that the total lift L is given and that the structural constraint $\bar{M}$ is given as well. Assume also that a lift distribution $\ell(s)$

which satisfies these conditions and results in the minimum drag is also given. Now consider three discrete elements of variation, as depicted in figure 3. We have

$$\left.\begin{aligned} \delta L = 0 \; ; \quad & \delta \ell_1 \cos \theta_1 + \delta \ell_2 \cos \theta_2 + \delta \ell_3 \cos \theta_3 = 0 \\ \delta \bar{M} = 0 \; ; \quad & \delta \ell_1 m_1 + \delta \ell_2 m_2 + \delta \ell_3 m_3 = 0 \\ \delta D_i = 0 \; ; \quad & \delta \ell_1 \frac{w_1}{2V} + \delta \ell_2 \frac{w_2}{2V} + \delta \ell_3 \frac{w_3}{2V} = 0 \end{aligned}\right\} \tag{7}$$

Here the m_n are purely geometric functions involving the shape of the wing trace; they represent the contribution, of a lift element at position n, to the structural quantity $\bar{M}$. In case the bending moment at the wing root is specified and the wing is planar, then m_1 is simply equal to y_1, that is, the moment arm of the lift element ℓ_1. Similarly, if the integrated bending moment (Prandtl's criterion) is employed, the function m_1 becomes $[(1/2)y_1]^2$, or the second moment of the lift element ℓ_1.

In the third equation, the w_n refer to the "downwash" produced by the original distribution. The drag added by the distributions $\Delta\ell_1$, etc., will, of course, contain the drag of the original distribution. However, because of Munk's mutual-interference theorem the two interference terms are equal, and we need consider only the first one. There is, in addition, the drag of the added distribution alone, but this is proportional to the square of ℓ_1, ℓ_2, etc., and hence does not contribute to the first-order variation.

Since equations (7) must hold for all variations and all positions of the $\Delta\ell$'s we will write for the general solution:

$$\frac{w}{2V} = A \cos \theta + Bm(s,\theta) \tag{8}$$

In the case of a planar wing with the integrated bending moments specified, we have

$$\begin{aligned} \theta &= 0 \\ m &= y^2 \end{aligned} \tag{9}$$

hence,

$$\frac{w}{2V} = A + By^2 \tag{10}$$

and the induced downwash must vary parabolically along the span. This is Prandtl's result.

In case the dimensions and shape of the wing in front view are given, but no additional structural constraint is imposed, we have

$$\frac{w}{2V} = A \cos \theta \tag{11}$$

Problems of this type are treated in reference 8. For a wing with vertical fins we find that $w = 0$ (zero "sidewash") over the fins in agreement with the classical treatments of this problem.

The solution of the variational problem does not give the load distribution for minimum drag directly, but gives instead the variation of downwash in the Trefftz plane in terms of the various constraint functions. It is then necessary to calculate the load distribution that is consistent with this downwash distribution — a standard problem in airfoil theory.

Although the theory can be applied to curved wing shapes, it is probably sufficient for practical reasons to consider wings composed of straight line segments, that is, a main wing panel and fins at each tip. Assume at first that the fins are vertical so that $\theta = 90°$ at the fins.

To derive the functions m_1, m_2, etc., in this case we first calculate the bending moment all along the span due to a lift element ℓ_1 at a position y_1 on the horizontal part of the wing. This gives

$$\delta M_1 = (y_1 - y)\delta \ell_1 \tag{12}$$

Integrating this over the semispan gives

$$\int M = \bar{M} = \frac{1}{2} y_1^2 \delta \ell_1 \tag{13}$$

so that within the horizontal portion of the wing

$$m = \frac{1}{2} y^2 \tag{14}$$

as before. For side-force elements $\delta \ell_2$ on the vertical fin the bending moment is

$$\delta M = (z_2 - z)\delta \ell_2 \tag{15}$$

Since the moment at the base of the fin ($z = 0$) is transmitted to the main wing spar, we have

$$\int_0^{s_t} \delta M \, ds = \left(\frac{1}{2} z_2^2 + y_t z_2\right)\delta \ell_2 \tag{16}$$

where y_t is the semispan. Collecting terms gives

$$m = \frac{1}{2} (y^2 + z^2) + y_t z \tag{17}$$

so that the downwash for minimum drag becomes

$$\frac{w}{2V} = A + B\left[\frac{1}{2}(y^2 + z^2) + y_t z\right] \tag{18}$$

The constants A and B will depend on the specified total lift and the specified average bending moment, $\bar{M}$. Because of the relation between the downwash and the structural criterion, the induced drag can be written

$$D_i = AL + B\bar{M} \tag{19}$$

Given the trace of the wing plus fins in the Trefftz plane and the velocity component w everywhere normal to the trace, we now have to obtain the solution of Laplace's equation in two dimensions with w as a boundary condition. The solution will give the potential jump $\Delta\phi$ across the wake, equal to the circulation around the wing. The method of solving this problem is given in the appendix.

Our calculations, based on lifting-line theory, do not give details of chordwise pressure or load distribution. It is important to realize, however, that calculations of induced drag by lifting-line theory are fully equivalent to those made by linear lifting-surface theory and are usually more accurate. In cases of wings having square or blunt tips, vortex roll-up will occur at high angles of attack and may lead to significant increases of drag over that given by the theory. For wings of high aspect ratio having rounded or elliptical tips, such nonlinear effects are negligible in the normal flight range.

In the case of unswept wings of high aspect ratio the downwash obtained by our formulas, w/2, can be applied at the wing and will give a distribution of twist angle consistent with the optimum loading. In the case of swept wings, however, additional twist angles are introduced by the sweep, and the wing twist required to produce the optimum loadings cannot be determined by simple lifting-line theory. The optimum span load distributions are not altered by sweep, although the appropriate structural criterion may be affected.

The induced drag is in principle not affected by the fore or aft positioning of the fin or winglet, although the camber and twist required to produce the ideal loadings will be altered. In the designs proposed by Whitcomb (ref. 1), the winglet is given a rearward position to avoid interference with the region of peak velocity on wing.

Figure 4 shows span load distributions calculated by our method for wings having winglets whose heights are 20 percent of the semispan. The load on the winglet is shown projected horizontally beyond the tip of the main wing. Assuming that each section operates at the same lift coefficient, the load curves are proportional to the chord length distribution for both wing and winglet. Calculations of induced drag, load distribution, and structural parameters remain unchanged if the wing system is inverted. The load on the downward projecting fin will then, of course, be directed outward.

Referring to figure 4, it appears that wing A, which has 0.9 the span of a comparable elliptic wing (i.e., an elliptic wing having the same lift and the same spar weight), will have the same induced drag $\left(D_i = D_{ie} = \frac{L^2}{\pi\rho/2V^2b^2}\right)$. Extending the wing to equal the span of the elliptic wing, but keeping the total spar weight (including winglet spar) the same, leads to a more highly tapered loading and an induced drag that is 0.89 that of the elliptic wing. With further increases of span, the taper becomes extreme and the load, together with the winglet, tends to disappear with no further reduction in drag.

Figure 5 shows the results of such calculations, for 10-percent and 20-percent winglets compared with those for flat wings, as a function of span ratio, using the elliptic wing as a basis. For span ratios less than 1, the wings (or load curves) become shorter and more blunt and the addition of winglets is surprisingly effective. However, the minimum drag that can be achieved by extending the span while keeping the spar weight constant seems to be about 0.89 D_{ie}, or the same as that obtained by Prandtl for flat wings. Hence, if our criterion of spar weight is adopted it appears that the addition of winglets cannot reduce the drag significantly below that of a flat wing having an ideal tapered planform and a span 10 percent greater than the ellipse (wing C, $b/b_e = 1.1$). However, the same drag value can be achieved without an increase of span by adding 15-percent winglets (a point slightly above wing B). For wings having planforms shorter than the ellipse and more blunt, the induced drag increases rapidly. In this region, however, the benefits of winglets are most pronounced.

Similar calculations, using different criteria for the structure weight, can be performed. Figure 6 shows the results obtained when the bending moment at a single point — the wing root — is used. In this case, it appears that a 15-percent reduction of induced drag below that of the elliptic wing can be achieved either by a flat wing or by wings with winglets, again with no decisive advantage for either type.

The foregoing results appear to be in disagreement with those of reference 9, which show a decisive advantage for winglets if the root bending moment is used as a criterion. The differences are probably attributable to our use of idealized wing shapes, which result in relatively narrow tip extensions, and the optimization of planform shape for each case.

APPENDIX

I. Introduction

We record here the more formal analysis upon which the results and discussion of the main text are based. In section II we derive the lift, drag, and integral bending moment expressions for wings with winglets at 90°. With these relations, a discussion of the variational problem for minimum induced drag is presented. Once the downwash and sidewash are specified by the variational problem, we determine the load distribution by considering the problem in the Trefftz plane. This is done in section III. Relations that lead to the comparison with the induced drag of elliptic wings (figs. 5, 6) are given in section IV. Although we restrict the present discussion to winglets at 90°, it should be emphasized that the techniques sketched below may be extended to treat winglets at any angle.

II. Minimum Induced Drag for Wings with 90° Winglets

We proceed by finding the lift, drag, and integral bending moment in terms of induced downwash and sidewash for the lifting-line geometry shown in figure 7. Using the Biot-Savart law, we find for the induced downwash $v_z(y)$ and sidewash $v_y(z)$

$$\left.\begin{aligned} v_z(y) \equiv v_z(x = 0, y, z = 0) &= \frac{1}{4\pi}\int_0^{z_\ell} \frac{d\Gamma}{dz}\left[\frac{(y - y_t)}{(y - y_t)^2 + z^2} - \frac{(y + y_t)}{(y + y_t)^2 + z^2}\right]dz \\ &+ \frac{1}{4\pi}\int_{-y_t}^{y_t} \frac{\frac{d\Gamma}{dy'}}{y - y'}\,dy' \\ v_y(z) \equiv v_y(x = 0, y = y_t, z) &= \frac{1}{4\pi}\int_0^{z_\ell} \frac{d\Gamma}{dz'}\left[\frac{1}{z' - z} + \frac{(z - z')}{(z' - z)^2 + 4y_t^2}\right]dz' \\ &+ \frac{z}{4\pi}\int_{-y_t}^{y_t} \frac{\frac{d\Gamma}{dy}}{(y + y_t)^2 + z^2}\,dy \end{aligned}\right\} \quad (A1)$$

Notice that the load distribution Γ is a function of both y and z. In (A1) we refer to $\Gamma(y = \pm y_t, z)$ for z integrations, and to $\Gamma(y, z = 0)$ for y integrations. By symmetry $v_y(x = 0, y = -y_t, z) = -v_y(z)$. The lift and induced drag are given by

$$L = \rho V \int_{-y_t}^{y_t} \Gamma(y)\,dy \tag{A2}$$

$$D = \rho \int_{-y_t}^{y_t} v_z(y)\Gamma(y)\,dy + 2\rho \int_{o}^{z_\ell} v_y(z)\Gamma(z)\,dz \tag{A3}$$

To compute the integral bending moment, we first find the bending moment at points along the wing-winglet trace. In vector notation, the bending moment at an arbitrary point s is written

$$\vec{M}(s) = \rho V \int_{s}^{s_t} (\vec{s}' - \vec{s}) \times \vec{\Gamma}(s')\,ds' \tag{A4}$$

where s_t denotes the wing tip. For the 90° winglet, we take

$$\vec{\Gamma}(s') = \begin{cases} + \Gamma(y')\hat{\vec{z}} & \text{for } 0 \le s' = y' \le y_t \\ - \Gamma(z')\hat{\vec{y}} & \text{for } 0 \le s' = z' \le z_\ell \end{cases} \tag{A5}$$

In the region $0 \le s = y \le y_t$, we have

$$\vec{M}(y) = \rho V \int_{y}^{y_t} (y' - y)\hat{\vec{x}} \times \vec{\Gamma}(y')\hat{z}\,dy' + \rho V \int_{o}^{z_\ell} [z'\hat{\vec{z}} + (y_t - y)\hat{\vec{y}}] \times [-\Gamma(z')\hat{\vec{y}}]\,dz'$$

$$= \hat{\vec{x}}\rho V \left[\int_{y}^{y_t} (y' - y)\Gamma(y')\,dy' + \int_{o}^{z_\ell} z\Gamma(z)\,dz \right] \equiv M(y)\hat{\vec{x}}$$

Similarly, in the region $0 \le s = z \le z_\ell$, we find

$$\vec{M}(z) \equiv M(z)\hat{\vec{x}} = \hat{\vec{x}}\rho V \int_{z}^{z_\ell} (z' - z)\Gamma(z')\,dz'$$

The integral bending moment is

$$\bar{M} = \int_{o}^{s_t} |\vec{M}(s)|\,ds = \int_{o}^{y_t} M(y)\,dy + \int_{o}^{z_\ell} M(z)\,dz$$

where $M(y)$ and $M(z)$ are given above. These integrals are easily evaluated; for example,

$$\int_o^{y_t} M(y)dy = yM(y)\Big|_o^{y_t} - \int_o^{y_t} y\,\frac{dM}{dy}\,dy$$

$$= y_t M(y_t) + \rho V \int_o^{y_t} y\left[\int_y^{y_t} \Gamma(y')dy'\right]dy$$

$$= \rho V y_t \int_o^{z_\ell} z\Gamma(z)dz + \rho V \int_o^{y_t} \frac{y^2}{2}\,\Gamma(y)dy$$

A similar calculation for $\int_o^{z_\ell} M(z)dz$ then yields

$$\bar{M} = \rho V \int_o^{y_t} \frac{y^2}{2}\,\Gamma(y)dy + \rho V \int_o^{z_\ell} \left(y_t z + \frac{z^2}{2}\right)\Gamma(z)dz \qquad \text{(A6)}$$

as found in equation (17) of the main text.

We may now formulate our minimum induced drag problem. We wish to find an extremum in the induced drag (A3) as a functional of the load distribution $\Gamma(y,z)$, subject to the constraint that the lift (A2) and integral bending moment (A6) be constant. Formally, we require that

$$\delta D - \lambda_L \delta L - \lambda_M \delta\bar{M} = 0 \qquad \text{(A7)}$$

where λ_L and λ_M are Lagrangian multipliers. Since L and $\bar{M}$ are "linear" in $\Gamma(y,z)$, their variations are simply

$$\delta L = \rho V \int_{-y_t}^{y_t} \delta\Gamma(y)dy$$

$$\delta\bar{M} = \frac{\rho V}{2} \int_{-y_t}^{y_t} \frac{y^2}{2}\,\delta\Gamma(y)dy + \rho V \int_o^{z_\ell} \left(y_t z + \frac{z^2}{2}\right)\delta\Gamma(z)dz \qquad \text{(A8)}$$

The variation of the induced drag is a more complicated calculation since the sidewash and downwash are themselves functionals of the load distribution. A straightforward, albeit tedious, calculation yields

$$\delta D = 2\left[\rho \int_{-y_t}^{y_t} v_z(y)\delta\Gamma(y)dy + 2\rho \int_o^{z_\ell} v_y(z)\delta\Gamma(z)dz\right] \qquad \text{(A9)}$$

Notice that this result is simply twice what we would find for the variation of D were $v_z(y)$ and $v_y(z)$ not functionals of $\Gamma(y,z)$; this is the essence of Munk's reciprocal theorem (ref. 2) for wings with 90° winglets. Combining equations (A7)-(A9), we have

$$\int_{-y_t}^{y_t} \left[2\rho v_z(y) - \lambda_L \rho V - \frac{\rho V}{2} \lambda_M \frac{y^2}{2}\right] \delta\Gamma(y)\,dy$$

$$+ \int_0^{z_\ell} \left[4\rho v_y(z) - \lambda_M \rho V\left(y_t z + \frac{z^2}{2}\right)\right] \delta\Gamma(z)\,dz = 0$$

Assuming $\Gamma(y,z)$ to be piecewise continuous, we conclude that

$$\left.\begin{aligned} v_z(y) &= \left(\frac{\lambda_L V}{2}\right) + \left(\frac{\lambda_M V}{4}\right)\frac{y^2}{2} \equiv A + B\,\frac{y^2}{2} \\ v_y(z) &= \left(\frac{\lambda_M V}{4}\right)\left(y_t z + \frac{z^2}{2}\right) \equiv B\left(y_t z + \frac{z^2}{2}\right) \end{aligned}\right\} \qquad \text{(A10)}$$

The parameters A and B of the text are effectively just the Lagrangian multipliers of our variational problem. Equation (A10) should be compared with equation (18) of the main text.

Although the above results are for 90° winglets, we note that they are readily generalized to winglets at any angle or to curved wing shapes.

III. Determination of the Load Distribution

The problem of determining the load distribution Γ such that the downwash and sidewash have the form (A10) is attacked in three stages:

1. The problem is first formulated in the Trefftz plane. Notice that (A10) specifies the stream function ψ at the wing-winglet surface. We seek the discontinuity in potential ϕ across that surface; it is proportional to the lift distribution.

2. We next map the wing-winglet into a straight line with a Schwarz-Christoffel transformation. The mapping is such that the analytic roles of ϕ and ψ are reversed, that is, ψ is discontinuous across the wing-winglet, and ϕ is now continuous.

3. In the transformed plane, a Cauchy integral relation yields the behavior of ϕ. Mapping back to the Trefftz plane and taking the discontinuity in ϕ yields the load distribution.

Our geometry for the Trefftz and transformed planes is presented in figure 8. Notice that we have stood the wing on its side and changed to the

notation commonly used in the complex plane. The symmetry of the wing about the x-axis (y = 0), both geometrically and analytically, should also be noted. The semispan is normalized to one (z = 0 to z = i) and the winglet has length x_ℓ (z = i to $z = -x_\ell + i$).

Expressed in the Trefftz or z-plane of figure 8, the constraint (A10) reads

$$\left.\begin{aligned} v_x &= A + B\,\frac{y^2}{2} = \frac{\partial \psi}{\partial y} \\ v_y &= B\left(-x + \frac{x^2}{2}\right) = -\frac{\partial \psi}{\partial x} \end{aligned}\right\} \tag{A11}$$

With the introduction of the complex potential

$$\Psi(z) = \phi(x,y) + i\psi(x,y)$$

it is implied by (A11) that

$$\psi(x,y) = Ay + B\left(\frac{y^3}{6} + \frac{x^2}{2} - \frac{x^3}{6}\right) \tag{A12}$$

on the lifting line. The desired load distribution is given by

$$\Gamma(x,y) = \frac{1}{2}\,(\phi_+ - \phi_-) \tag{A13}$$

where the subscripts (+,-) refer to the top (+) and bottom (-) of the lifting line. The factor of 2 is a normalization convenience; an elliptic wing would have $\Gamma = 1$ at the root.

We next map the z-plane into the ζ-plane (see fig. 8). The appropriate Schwarz-Christoffel transformation is

$$z(\zeta) = A \int_{-1}^{\zeta} \frac{(t - c)^{1/2}(t + b)}{(t + a)^{1/2}(t + 1)^{1/2}(t - 1)^{1/2}}\,dt \tag{A14}$$

subject to the constraints

$$\left.\begin{aligned} z(-1) &= 0 \\ z(-a) &= i \\ z(-b) &= -x_\ell + i \\ z(+c) &= i \\ z(1) &= 0 \end{aligned}\right\} \tag{A15}$$

By convention, we take the parameters A, a, b, c to be positive. The integral (A14) is computed using Simpson's rule. In the vicinity of points where the integrand is singular, the following procedure is used. Consider the integral

$$z(\zeta) = \int_{-1}^{\zeta} \frac{g(t)}{(t+1)^{\alpha}}\, dt$$

where $g(-1)$ is finite and

$$\lim_{t \to -1} \left[\frac{g(t) - g(-1)}{(t+1)^{\alpha}} \right] = 0$$

This latter relation will generally hold for any transformation where $0 < \alpha < 1$; in particular, we could consider wings with winglets at any angle. We evaluate $z(\zeta)$ with

$$z(\zeta) = \int_{-1}^{-1+\delta} \frac{[g(t) - g(-1)]}{(t+1)^{\alpha}}\, dt + \frac{1}{\alpha}\, g(-1)\delta^{\alpha} + \int_{-1+\delta}^{\zeta} \frac{g(t)}{(t+1)^{\alpha}}\, dt \qquad \text{(A16)}$$

The remaining integrals may then be evaluated using Simpson's rule, the singularity having been removed from the regions of integration.

The parameters A, a, b, and c are found by numerically solving the nonlinear equations

$$\left.\begin{aligned} \text{Re } z(-b) &= -x_{\ell} \\ \text{Im } z(-b) &= 1 \\ \text{Re } z(1) &= 0 \\ \text{Im } z(1) &= 0 \end{aligned}\right\} \qquad \text{(A17)}$$

The resulting mappings were in general accurate to about one part in a million. A further check was provided by comparison with the results of Faulkner and Darwin (ref. 4) who evaluated (A14) using elliptic functions.

As noted earlier, the discontinuity of $\Psi(\zeta)$ across the $\eta = 0$ line for $-1 \le \zeta \le 1$ is given by $\psi(\xi,0)$. A simple application of Cauchy's theorem to $\Psi(\zeta)$ then yields

$$\phi(\xi) = \frac{P}{\pi} \int_{-1}^{1} \frac{\psi(t)}{t - \xi}\, dt \qquad \text{(A18)}$$

where $\phi(\xi)$ and $\psi(t)$ indicate values of ϕ and ψ on the $\eta = 0$ line. This expression is valid up to the usual polynomial ambiguity. We define two potentials corresponding to the Lagrangian multipliers A and B (cf. (A10) and (A12))

$$\phi_A(\xi) = \frac{P}{\pi} \int_{-1}^{1} \frac{y(t)dt}{t - \xi} \tag{A19}$$

$$\phi_B(\xi) = \frac{P}{2\pi} \int_{-1}^{1} \left[x^2(t) - \frac{1}{3} x^3(t) + \frac{1}{3} y^3(t)\right] \frac{dt}{t - \xi} \tag{A20}$$

In (A19) and (A20), the values of x and y are given by (A14). Notice that the potential ϕ_A corresponds to minimum drag with only the constant lift constraint; this is the problem solved by Faulkner and Darwin (ref. 4) for winglets at 90°. The potential ϕ_B reflects the additional constraint of constant integral bending moment.

The numerical evaluation of the principal valued integrals (eqs. (A19), (A20)) is reasonably straightforward. The behavior of $y(\xi)$ and $x(\xi)$ for a 20-percent winglet is shown in figure 9. Besides subtracting off the logarithmic variation due to the principal value, for example,

$$\phi_A(\xi) = \frac{1}{\pi} \int_{-1}^{1} \frac{[y(t) - y(\xi)]}{t - \xi} dt + \frac{y(\xi)}{\pi} \ln \left|\frac{1 - \xi}{1 + \xi}\right|$$

we also used a method similar to that of (A16) to handle "cusp points" in the behavior of $y(\xi)$.

For unit constant downwash in the Trefftz plane, the analytic solution for ϕ_A is given by

$$\phi_A(\xi) = \text{Re } z(\xi) - A\xi \tag{A21}$$

where A is the mapping parameter in (A14). In figure 10 we compare this result with our numerical evaluation of ϕ_A. Notice that the abscissa corresponds to the wing and winglet as denoted by "y" and "x" (see, also, fig. 7). The two curves agree up to an offset of -0.041. This value is just the limit of (A21) as $\xi \to \infty$. Recall that the Cauchy relation (A18) must be modified by adding a polynomial $P_n(\xi)$ when

$$\Psi(\zeta) \xrightarrow[|\zeta| \to \infty]{} P_n(\zeta)$$

Thus, the offset in figure 10(a) is expected when we use (A18). Notice that this constant will have no effect on the value of the corresponding load distribution. The behavior of ϕ_B is shown in figure 10(b). We suspect that its absolute value is offset as for ϕ_A.

The load distributions are found from ϕ_A and ϕ_B with

$$\Gamma_A = \frac{1}{2}(\phi_{A+} - \phi_{A-})$$

$$\Gamma_B = \frac{1}{2}(\phi_{B+} - \phi_{B-})$$

where the subscripts (+,-) denote values of ϕ above and below the abscissa in figure 10. These load distributions are shown in figure 11. In practice, only discrete points for ϕ_A and ϕ_B, not continuous curves, are obtained. The calculation of Γ_A and Γ_B thus requires the interpolation of values for $\phi_{A\pm}$ and $\phi_{B\pm}$ at corresponding abscissa points.

IV. Induced-Drag Comparison

We may now derive the expressions that give the induced-drag ratio D_i/D_{ie} shown in figures 5 and 6. By requiring that the wing with winglets have the same lift and integral bending moment as an elliptic wing, we find for the parameters A and B (recall (A10))

$$\left.\begin{aligned} A &= \frac{\pi}{4}\left(\frac{b_e}{b}\right)^2\left[M_B - \frac{L_B}{8}\left(\frac{b_e}{b}\right)^2\right]\Big/(L_A M_B - L_B M_A) \\ B &= \frac{\pi}{4}\left(\frac{b_e}{b}\right)^2\left[-M_A + \frac{L_A}{8}\left(\frac{b_e}{b}\right)^2\right]\Big/(L_A M_B - L_B M_A) \end{aligned}\right\} \tag{A22}$$

the factor $\pi/4$ corresponds to taking

$$\Gamma_e(y) = (1 - y^2)^{1/2}$$

for the elliptic wing with the semispan $b_e/2$ normalized to $y = 1$. The quantities L_A, L_B, M_A, M_B are simply moments of Γ_A and Γ_B as determined in section III:

$$\left.\begin{aligned} L_A &= \int_o^1 \Gamma_A(y)\,dy \;, \quad L_B = \int_o^1 \Gamma_B(y)\,dy \\ M_A &= \int_o^1 \Gamma_A(y)\,\frac{y^2}{2}\,dy + \int_o^{x_\ell}\left(x + \frac{x^2}{2}\right)\Gamma_A(x)\,dx \\ M_B &= \int_o^1 \Gamma_B(y)\,\frac{y^2}{2}\,dy + \int_o^{x_\ell}\left(x + \frac{x^2}{2}\right)\Gamma_B(x)\,dx \end{aligned}\right\} \tag{A23}$$

Once Γ_A and Γ_B are known, the parameters A and B may be considered functions of the ratio b_e/b. The induced-drag ratio is then given by

$$\frac{D_i}{D_{ie}} = \frac{4}{\pi}\left(\frac{b}{b_e}\right)^2 [A^2 L_A + AB(L_A + M_B) + B^2 M_B] \tag{A24}$$

In deriving (A22)-(A24), we note that lift and drag scale as b^2, whereas the integral bending moment scales as b^4.

In the case of a straight wing, the formalism discussed in this appendix was used to solve the Prandtl problem (ref. 6) as well as that posed in reference 7. All the calculations can be done in "closed form"; they yielded the same results as in references 6 and 7. To check our accuracy, this exercise was also done using the numerical techniques described above for evaluating the various integrals involved. The two methods of calculation agreed to better than a tenth of a percent.

REFERENCES

1. Whitcomb, Richard T.: A Design Approach and Selected Wind Tunnel Results at High Subsonic Speeds for Wing Tip Mounted Winglets. NASA TN D-8260, 1976.

2. Munk, Max M.: The Minimum Induced Drag of Aerofoils. NACA TR-121, 1921. (Reprinted in — Jones, R. T., ed.: Classical Aerodynamics Theory. NASA RP-1050, 1979.)

3. Hemke, Paul E.: Drag of Wings with End Plates. NACA TR-267, 1927.

4. Faulkner, V. M.; and Darwin, C.: The Design of Minimum Drag Tip Fins. A.R.C. Technical Report, R. & M. No. 2279, 1945.

5. Faulkner, V. M.; and Darwin, C.: The Design of Minimum Drag Inboard Fins. Br. A.R.C. Technical Report, R. & M. No. 2280, 1945.

6. Prandtl, L.: Über Tragflügel des Kleinsten Induzierten Widerstandes. Zeitschrift für Flugtechnik und Motorluftschiffahrt 24 Jg. 1933. (Reprinted in — Tollmien, W.; Schlichting, H.; and Görtler, H., eds: Gesammelte Abhandlungen. Springer-Verlag, 1961.)

7. Jones, Robert T.: The Spanwise Distribution of Lift for Minimum Induced Drag of Wings Having a Given Lift and a Given Bending Moment. NACA TN-2249, 1950. (See also Klein, A.; and Viswanathan, S. P.: Minimum Induced Drag of Wings with Given Lift and Root Bending Moment. ZAMP, vol. 24, Dec. 1973.)

8. Cone, Clarence D., Jr.: Theory of Induced Lift and Minimum Induced Drag of Nonplanar Lifting Systems. NASA TR-R139, 1962.

9. Heyson, H. H.; Riebe, G. D.; and Fulton, C. L.: Theoretical Parametric Study of the Relative Advantages of Winglets and Wing-Tip Extensions. NASA TM X-74003, 1977.

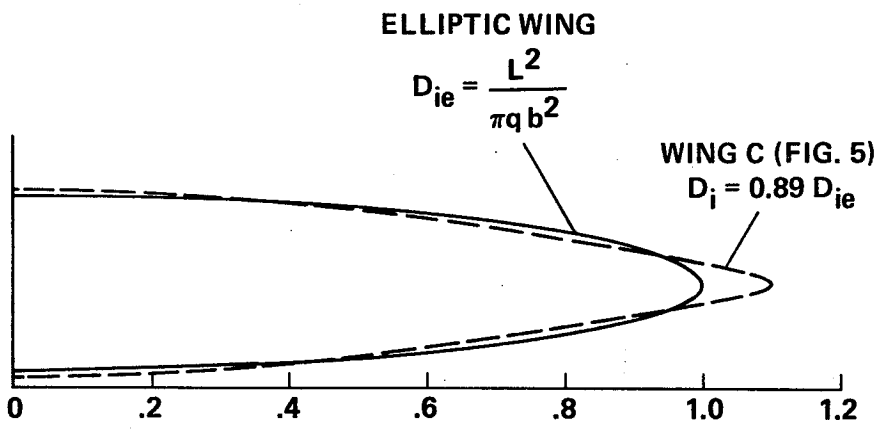

Figure 1.- Planar wings having equal spar weight according to Prandtl's criterion.

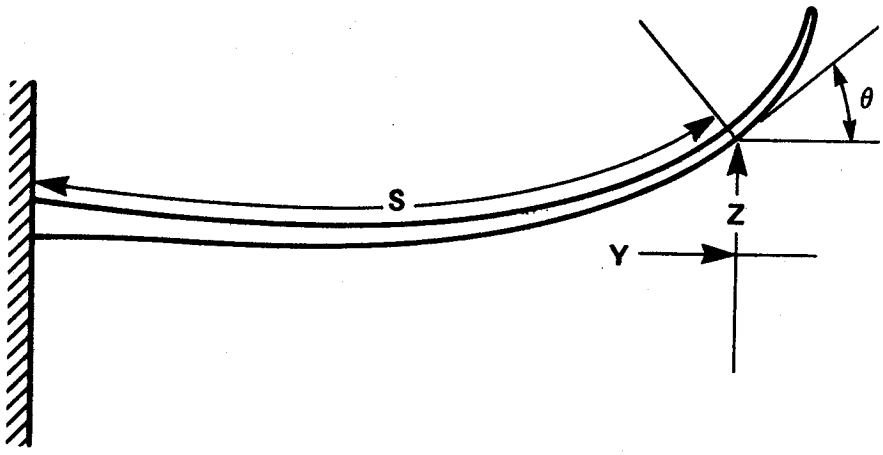

Figure 2.- Coordinates of nonplanar wing.

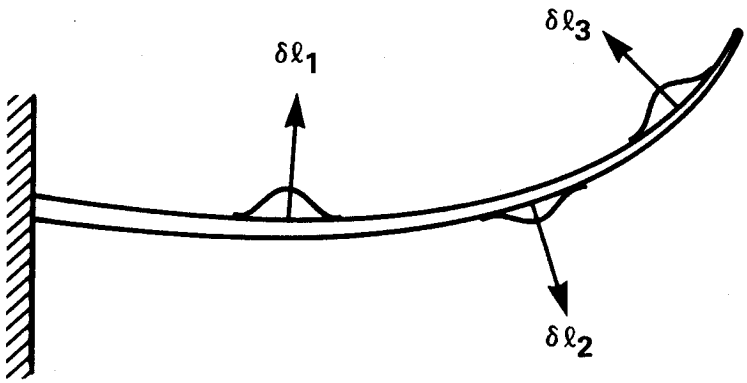

$$\delta\ell_1 \cos\theta_1 + \delta\ell_2 \cos\theta_2 + \delta\ell_3 \cos\theta_3 = 0$$

$$\delta\ell_1 m_1 + \delta\ell_2 m_2 + \delta\ell_3 m_3 = 0$$

$$\delta\ell_1 \frac{w_1}{2V} + \delta\ell_2 \frac{w_2}{2V} + \delta\ell_3 \frac{w_3}{2V} = 0$$

Figure 3.- Variational problem.

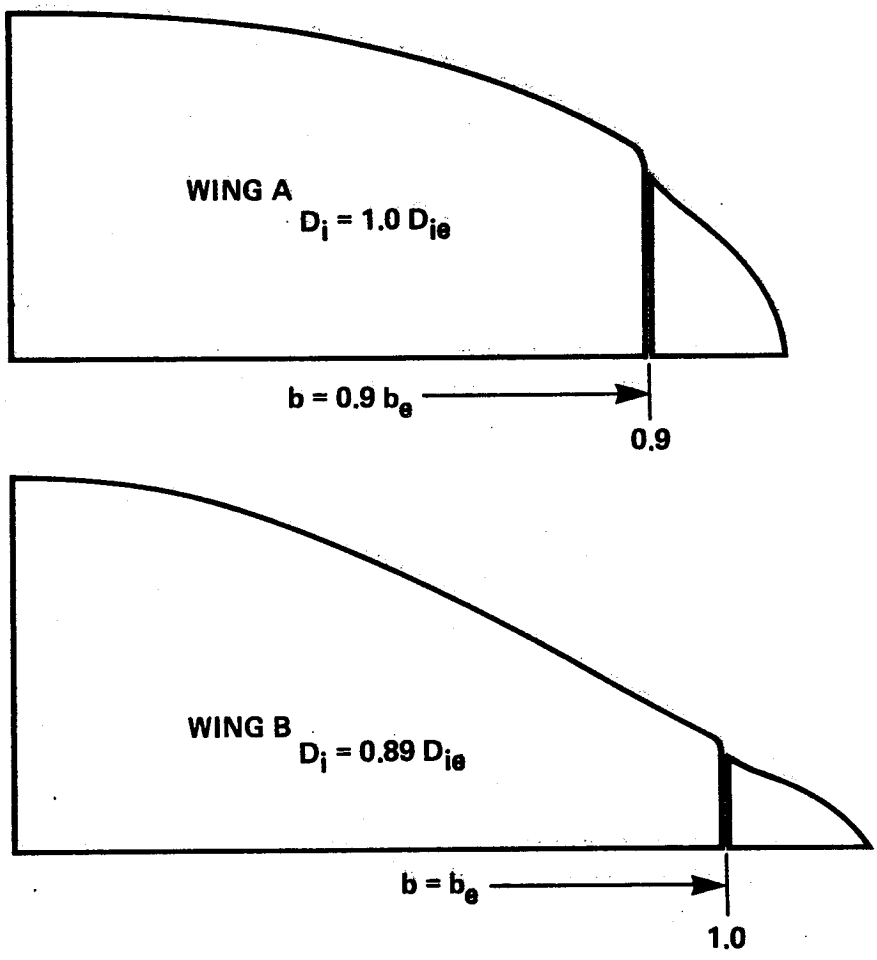

Figure 4.- Load curves for wings with winglets.

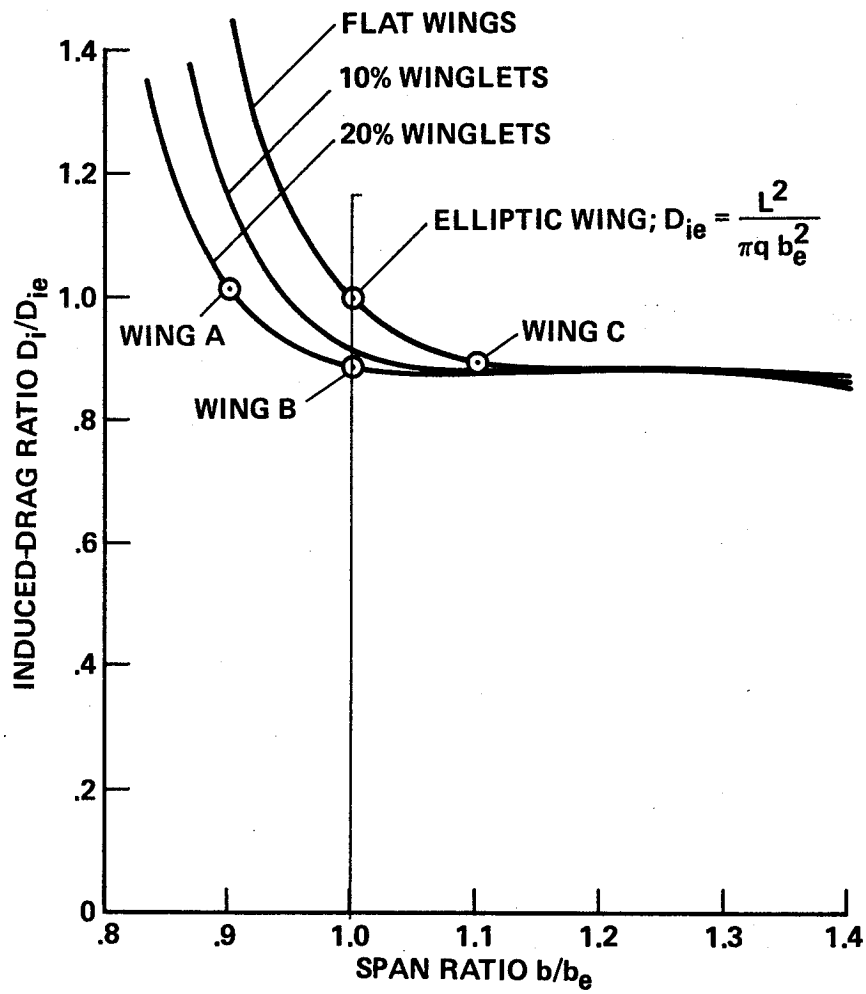

Figure 5.- Induced drag of wings having the same integrated moment $\bar{M}$.

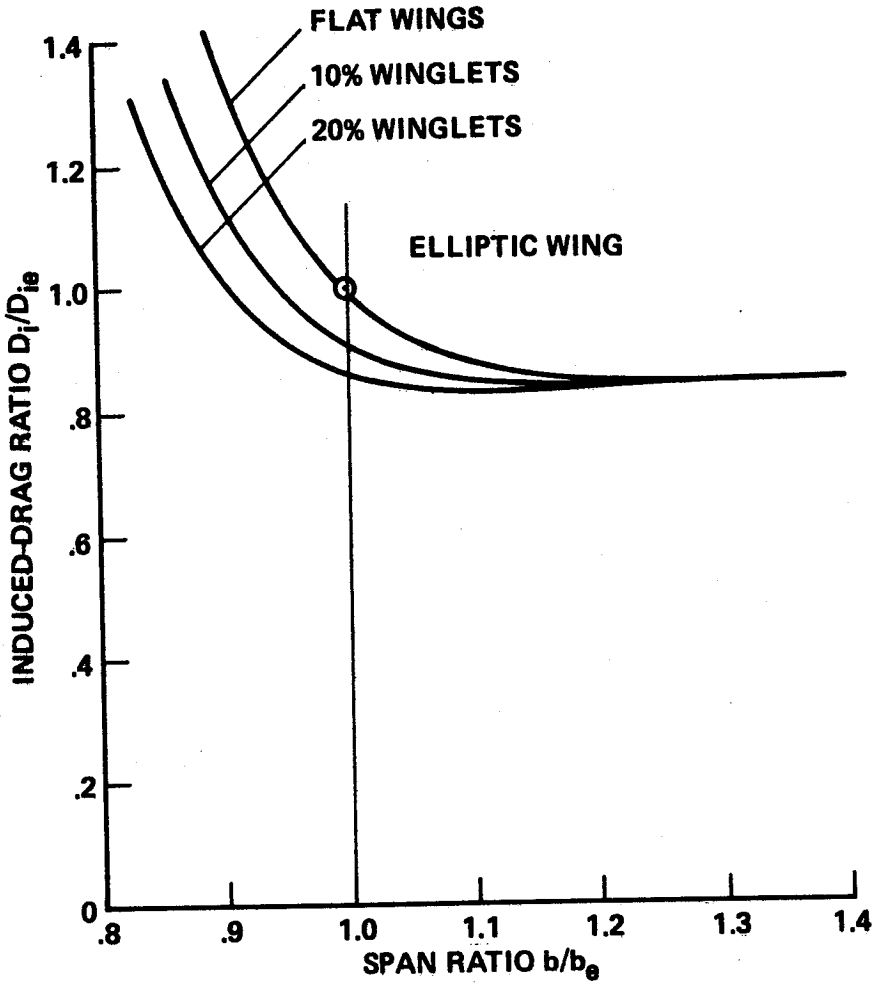

Figure 6.- Induced drag of wings having the same bending moment at the wing root.

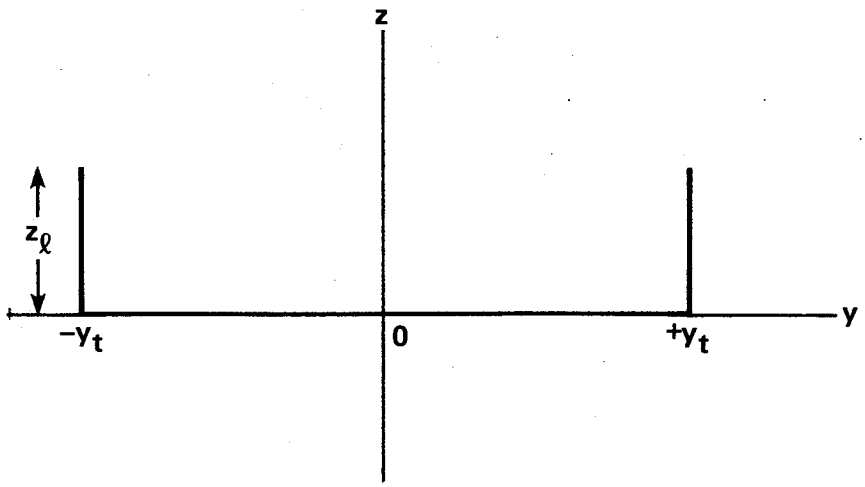

Figure 7.- Lifting-line geometry for wing with 90° winglets (x = 0 plane).

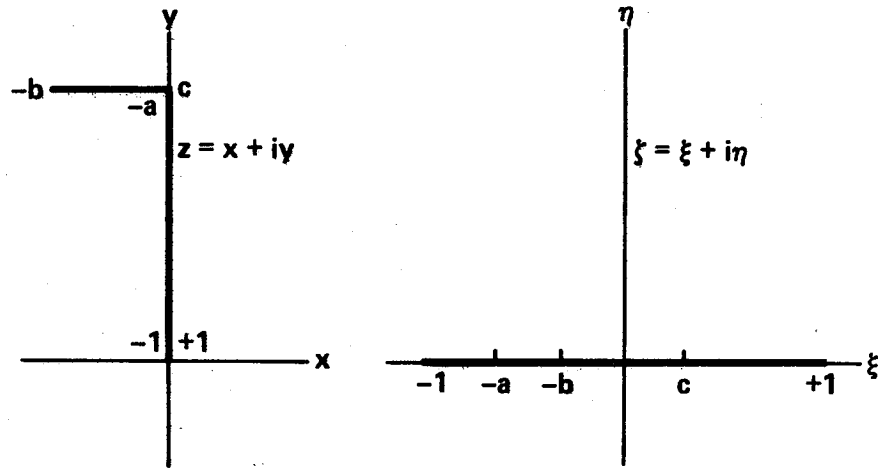

Figure 8.- Transformation of wing-winglet in the Trefftz plane into a straight line; corresponding points are labeled -1, -a, -b, c, +1.

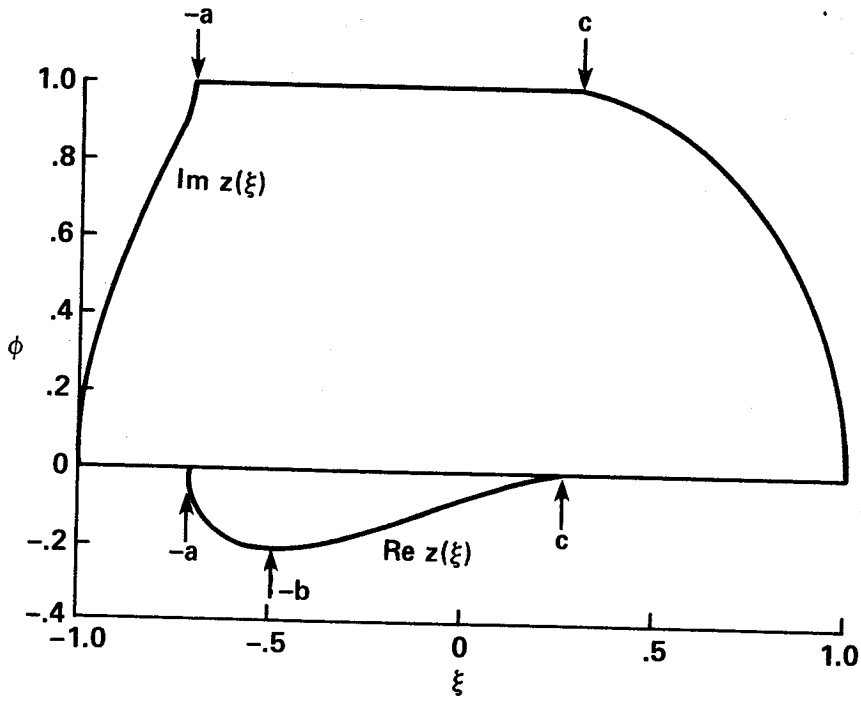

Figure 9.- Behavior of $y = \text{Im } z(\xi)$ and $x = \text{Re } z(\xi)$ for a 20-percent winglet ($x_\ell = 0.2$); the mapping constants are $A = 1.1195$, $a = 0.7110$, $b = 0.4924$, $c = 0.2739$.

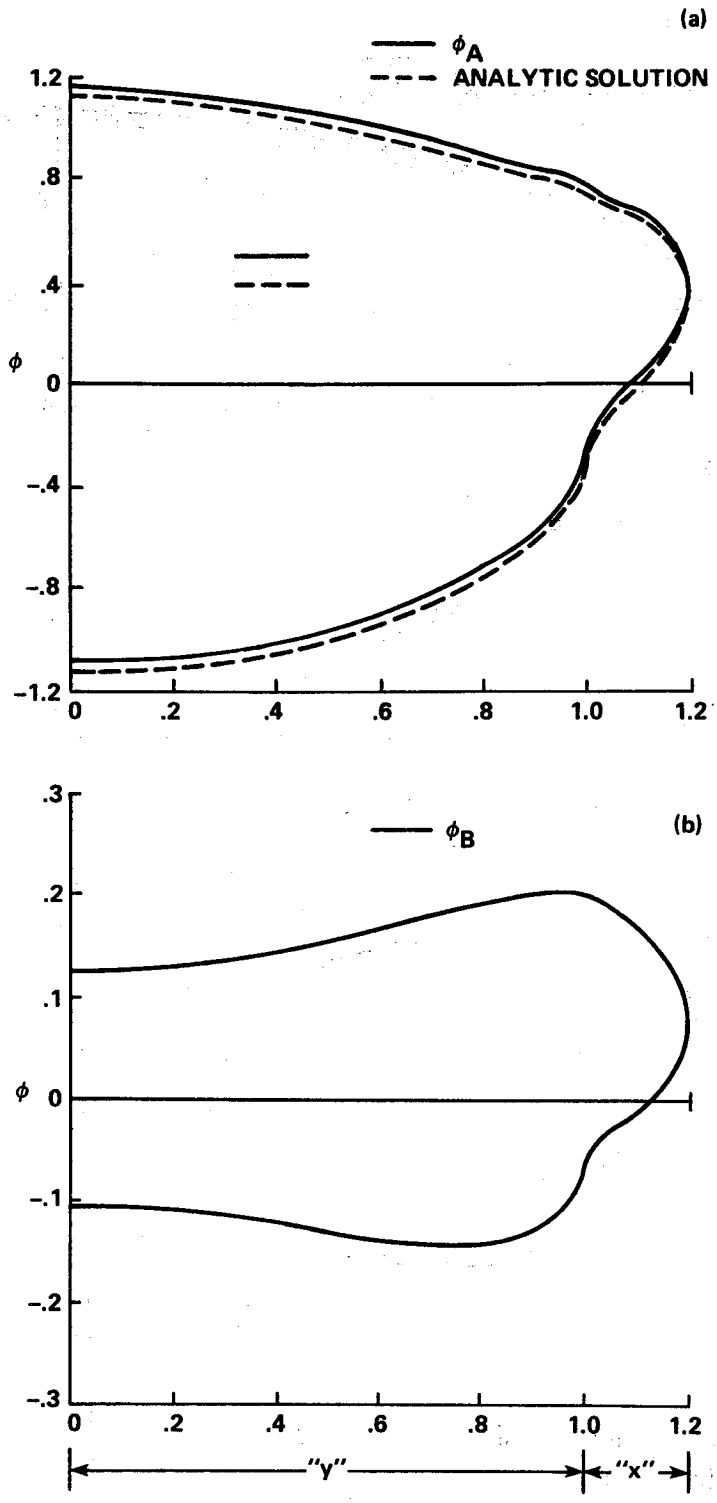

Figure 10.- Potential distributions for wing with winglets.

(a) Comparison of numerical evaluation of ϕ_A with the analytic solution for a 20-percent winglet; "y" denotes wing and "x" denotes winglet. The constant offset of 0.041 is just the limit of $z(\xi) - A\xi$ as $\xi \to \infty$.

(b) The potential ϕ_B corresponding to the integral bending moment constraint.

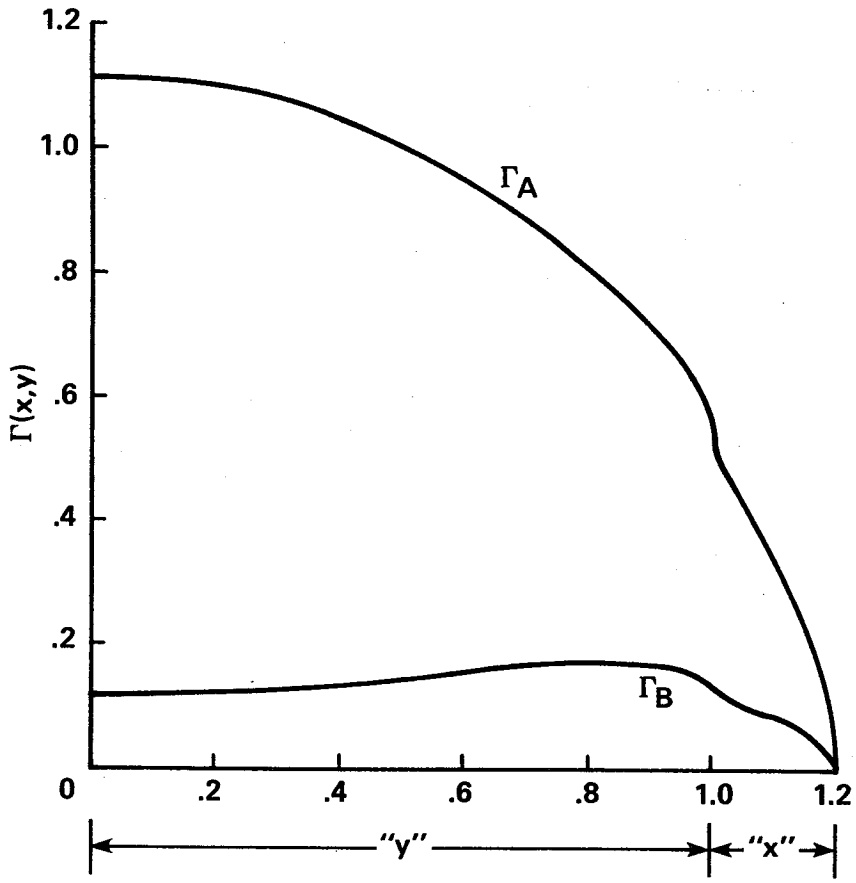

Figure 11.- Load distributions for 20-percent winglets; Γ_A corresponds to constant downwash, Γ_B to the integral bending moment constraint.